APPLICATION OF MODELS FOR ELECTRICAL ENERGY CONSUMPTION TO IMPROVE EAF OPERATION AND DYNAMIC CONTROL

Dr.-Ing. Bernd Kleimt, Betriebsforschungsinstitut, Düsseldorf, Germany
Dr.-Ing. Siegfried Köhle, Hilden, Germany
Dr.-Ing. Robert Kühn, Georgsmarienhütte, Germany
Dipl.-Ing. Sven Zisser, Betriebsforschungsinstitut, Düsseldorf, Germany

ABSTRACT

Within this paper, different approaches and models for an energy balance of an electric arc furnace are described. With a formula for calculation of the electrical energy demand, which was developed by statistical analysis of data from more than 50 furnaces, the electrical energy consumption of a furnace can be assessed and analysed in comparison to other furnaces. At the DC furnace of Georgsmarienhütte (GMH) an extensive data acquisition including permanent off-gas analysis is used for an on-line differential energy balance. A synthesis of both modelling approaches was used to derive a complete dynamic energy and mass balance model, which has been tested and verified with data from the GMH furnace. The described models can be used as tools to improve EAF operation and dynamic control.

INTRODUCTION

A formula for calculating the electrical energy demand of arc furnaces had been developed by statistical analysis of average values from more than 50 furnaces. As reported at the preceding Electric Steelmaking Conference in Venice 2002, that formula was extended and improved on the basis of single heat values for more than 5000 heats from 5 furnaces, as well as monthly average values for one of them over 3 years [1]. With this statistical model, the electrical energy consumption of a furnace can be assessed in comparison to other furnaces, and variations of electrical energy consumption at the same furnace can be analysed. Effects on electrical energy consumption and on furnace productivity have been determined for the influencing variables of the energy demand formula [2].

For calculating the electrical energy demand, the formula includes gas and oxygen consumption with respect to related chemical energy input. Concerning energy losses by vessel cooling and gas exhaustion, if measured at a furnace, the formula only regards the deviation of losses for an individual heat from their mean value over all heats of the furnace. For an energy balance however, the energy losses have to be included as absolute values, and further sources of chemical energy input must be respected, i.e. combustion with oxygen from entrained air as well as slag reactions. With help of the energy demand formula, more than 200 kWh/t can be estimated for this additional energy input [3].

For on-line process observation and control on basis of an energy balance, this one has to be cyclically calculated from measured values. Energy losses by gas exhaustion can be determined from the water flow rate and temperature difference in the water cooled exhaust gas duct, together with the gas flow rate and temperature measured behind, if post-combustion is completed there [4]. With measurement of the composition and the flow rate of the off-gas, its sensible and chemical heat contents can be distinguished, and post-combustion within the furnace can be observed.

ELECTRICAL ENERGY DEMAND FORMULA

The formula for calculating the electrical energy demand of arc furnaces is given in **Table 1** [1]. It takes into account specific consumption of total and several individual ferrous materials, slag formers, burner gas, oxygen for blowing by lance as well as for post-combustion, temperature before tapping and tap-to-tap time, divided in power-on and power-off time. All consumption values - also the electrical energy consumption for comparison with the calculated demand - are related to the tap weight, i.e. the weight of steel in the ladle per heat, including ferroalloys added at tapping.

Table 1: Formula for electrical energy demand of arc furnaces

$$\frac{W_R}{kWh/t} = 375 + 400 \cdot \left[\frac{G_E}{G_A} - 1\right] + 80 \cdot \frac{G_{DRI/HBI}}{G_A} - 50 \cdot \frac{G_{Shr}}{G_A} - 350 \cdot \frac{G_{HM}}{G_A} + 1000 \cdot \frac{G_Z}{G_A}$$

$$+ 0.3 \cdot \left[\frac{T_A}{°C} - 1600\right] + 1 \cdot \frac{t_S + t_N}{min} - 8 \cdot \frac{M_G}{m^3/t} - 4.3 \cdot \frac{M_L}{m^3/t} - 2.8 \cdot \frac{M_N}{m^3/t} + NV \cdot \frac{W_V - W_{Vm}}{kWh/t}$$

G_A	furnace tap weight	t_S	power-on time
G_E	weight of all ferrous materials	t_N	power-off time
G_{DRI}	weight of DRI	M_G	specific burner gas
G_{HBI}	weight of HBI	M_L	specific lance oxygen
G_{Shr}	weight of shredder	M_N	specific post-combustion oxygen
G_{HM}	weight of hot metal	W_V	energy losses (if measured)
G_Z	weight of slag formers	W_{Vm}	mean value of W_V
T_A	tapping temperature	NV	furnace specific factor (0.2 ... 0.4)

For measured energy losses by vessel cooling and gas exhaustion, the deviation for an individual heat from the mean value over all heats is taken into account by the factor NV, which has to be determined specifically for each furnace. As the mean value of the electrical energy demand is thus not effected by the energy losses, furnaces with and without measurement of these losses can be compared in evaluating their electrical energy consumption. For an individual furnace however, variation in energy losses from heat to heat may explain a considerable part of the variation in electrical energy consumption [2].

Monitoring of performance improvement at an electric arc furnace

For an AC furnace with a tap weight of 80 t and 70 MVA apparent power, monthly averages of electrical energy consumption are presented in **Fig. 1**. The calculated demand is in very good accordance to the actual consumption with a high correlation coefficient of 92 %. The calculation error has a mean value of 2 kWh/t and a standard deviation of 7 kWh/t.

The reduction of electrical energy consumption by about 40 kWh/t was achieved by increasing the share of shredded scrap, by higher burner gas and oxygen input, and by lower consumption of slag formers [2].

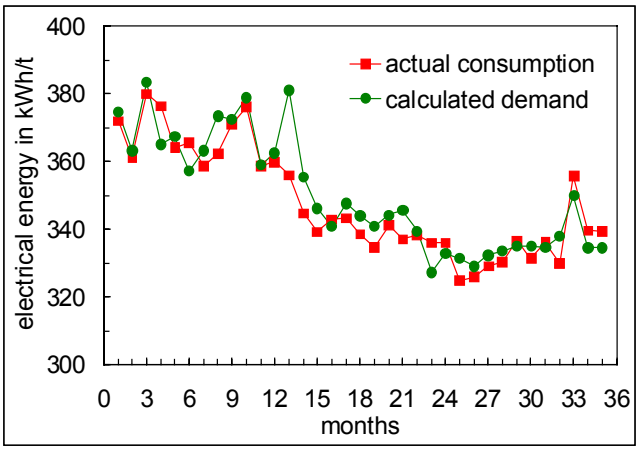

Fig. 1: Reduction of electrical energy consumption at a furnace over 3 years

Effects on electrical energy consumption and furnace productivity

For investigating effects on electrical energy consumption and productivity, a furnace with reference data from **Table 2** is assumed. With the electrical energy consumption W_E, the specific electric power (P_S/G_A) at main melting and its mean utilisation degree N_P during power-on, the power-on time

$$t_S = \frac{W_E \cdot G_A}{N_P \cdot P_S} = \frac{W_E}{N_P \cdot (P_S / G_A)} \qquad (1)$$

of 44.7 min is calculated.

The power-off time is chosen to give a tap-to-tap time of 60 min. With the tap weight of 150 t, the productivity

$$P_R = \frac{G_A}{t_S + t_N} \qquad (2)$$

is 150 t/h. After substituting t_S by equ. (1) it becomes obvious, that the productivity

$$P_R = \frac{N_P \cdot P_S}{W_E + N_P \cdot (P_S / G_A) \cdot t_N} \qquad (3)$$

Table 2: Reference data for the investigation

electrical energy consumption	W_E	380	kWh/t
specific power at main melting	P_S/G_A	600	kW/t
power utilisation degree	N_P	0.85	
➔ power-on time	t_S	44.7	min
power-off time	t_N	15.3	min
➔ tap-to-tap time	t_S+t_N	60	min
tap weight	G_A	150	t
➔ furnace productivity	P_R	150	t/h

mainly depends on the mean electric power, the electrical energy consumption and the power-off time, whereas the tap weight has a second order influence.

When by means of equ. (1) the power-on time is eliminated from the electrical energy demand formula, W_R gets the specific power (P_S/G_A) as a new influencing variable. Derivatives of W_R for its variables describe their effects on electrical energy consumption. These effects are shown by the left columns in **Fig. 2** for variations of influencing variables as given in the figure [2].

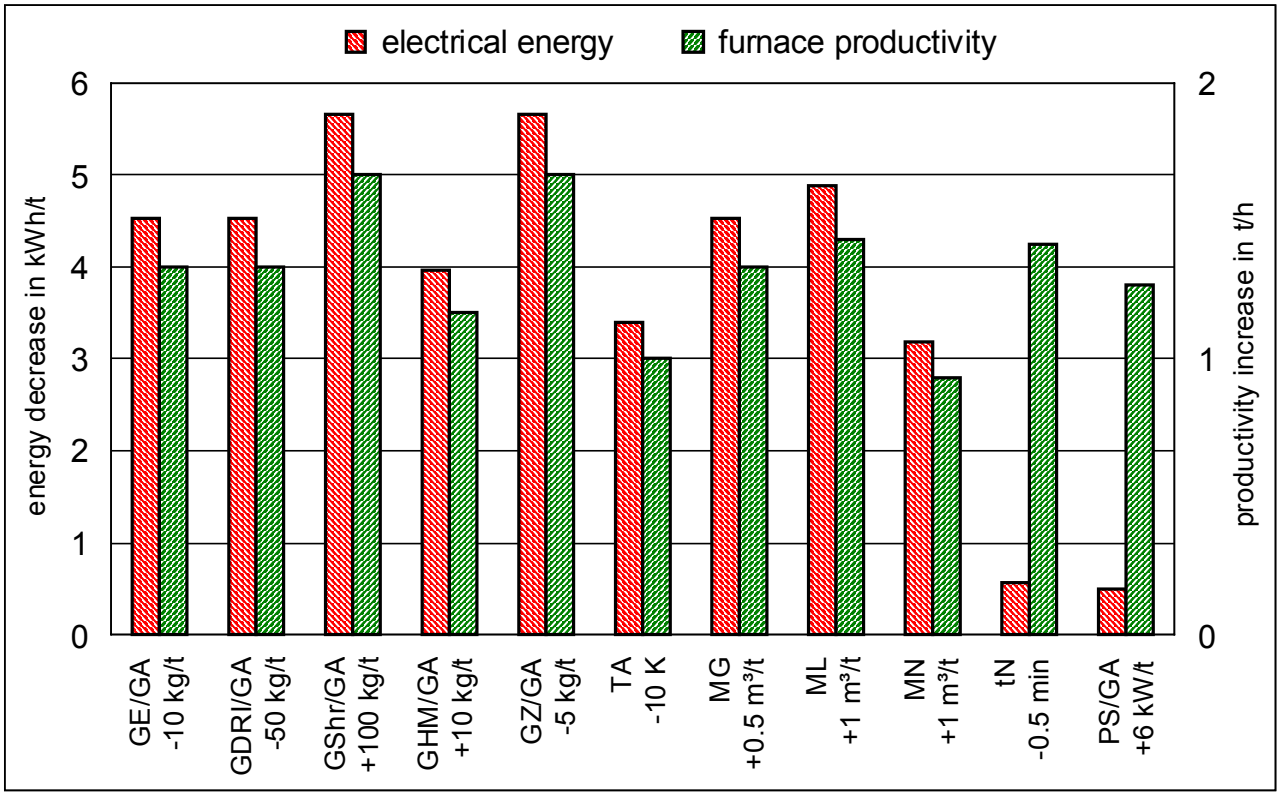

Fig. 2: Effects of varied influencing variables on electrical energy consumption and productivity (variables in Table 1, specific power P_S/G_A at main melting, reference data in Table 2)

The right columns in Fig. 2 represent the corresponding effects on furnace productivity, resulting from derivatives of P_R from equ. (2, 3) for the individual variables [2]. For most of them, both effects are proportional to each other by the ratio dP_R/dW_E = -0.294 (t/h)/(kWh/t) for the assumed reference data. The power-off time t_N and the specific electric power (P_S/G_A) have low effects on the electrical energy consumption of a furnace, but both of them strongly influence its productivity.

APPLICATION OF ENERGY BALANCE CALCULATIONS AT THE GMH DC FURNACE

Georgsmarienhütte (GMH) operates a 130t DC-EAF with a power rating of 130 MVA. Tap to tap time is about 65 min, power on time is 50 min. The layout of the furnace is shown in **Fig. 3**. Fossil energies are added as charge coal with the scrap bucket and blowing coal via a lance. The furnace is equipped with four natural gas/oxygen burners. Two of them can be operated as jet, i.e. a coherent supersonic oxygen stream is used to refine the steel melt. Additional oxygen is supplied by two consumable door lances and two subsonic injectors in the furnace wall, the latter ones mainly for post combustion.

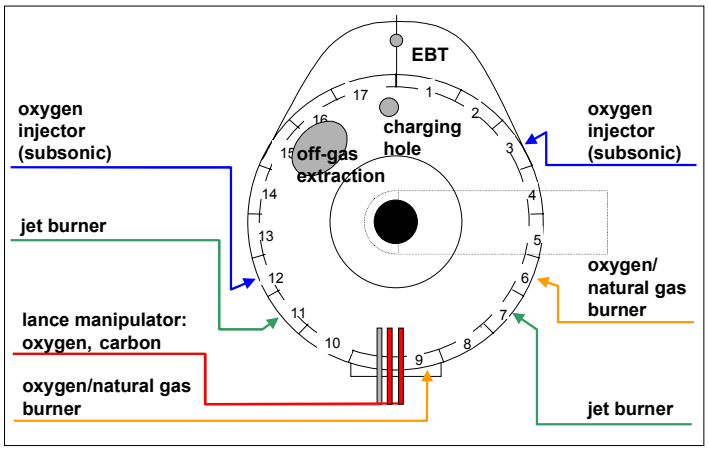

Fig. 3: Layout of GMH furnace

Calculations with the electrical energy demand formula

For the DC EAF of GMH, calculations with the formula for the electrical energy demand were performed to asses the efficiency of energy input in comparison to other furnaces. For this purpose, the process data of 200 single heats treated under standard operating conditions were evaluated. Furthermore the results of 60 trial heats under a nearly airtight furnace condition were provided. Although for these trial heats the lance manipulator was still used for oxygen injection, the furnace door was closed almost completely during lance operation, leaving only a small gap for introduction of the lance tip. **Table 3** shows the average model input values of the GMH heats for the standard and the nearly airtight operation, according to the naming scheme given in Table 1.

Table 3: Average values of input variables for electrical energy demand calculation of GMH heats with standard and nearly airtight operating conditions

Variable	W_R	W_E	G_A	g_E	g_{HBI}	g_Z	T_A	t_S	t_N	M_G	M_L	M_N
Unit	kWh/t	kWh/t	t	kg/t	kg/t	kg/t	°C	min	min	m³/t	m³/t	m³/t
Standard operation	447	492	130	1142	---	38	1653	52	20	3.5	16.4	3.1
Airtight operation	455	484	129	1157	15	48	1672	49	17	3.8	18.6	3.2

In **Fig. 4** the electrical energy demand W_R calculated according to the formula is plotted against the actual electrical energy consumption W_E for the single heat values of the GMH furnace under standard and nearly airtight operating conditions. The actual electrical energy consumption is significantly higher than the calculated demand. The modelling error, i.e. the difference between calculated demand and actual consumption, has for the standard heats a mean value of - 45 kWh/t, for the heats under airtight conditions the mean value is only - 29 kWh/t.

A correlation analysis between the calculated energy demand and its difference to the actual consumption on the one hand, and the considered influence parameters on the other hand revealed that the energetic yield of the oxygen injected into the bath is not as high as expected within the model. The reason is that obviously the combustion of the injected and charged carbon is not efficient for all heats, which results in a low post combustion ratio. This will be shown in the following for an example heat.

The heats performed under nearly airtight conditions show no significant difference in the electrical energy consumption compared to the standard conditions. However, it has to be noted that for the trial heats HBI was used as a part of the metallic charge material, which has a higher specific energy consumption. Furthermore the tapping temperature was slightly higher, and a higher amount of slag formers was used.

The calculation with the formula for the electrical energy demand allows to compare the overall energy consumption of the two operation practices. The difference of 16 kWh/t of the mean modelling errors can be regarded as energy saving which is due to the airtight operation practice.

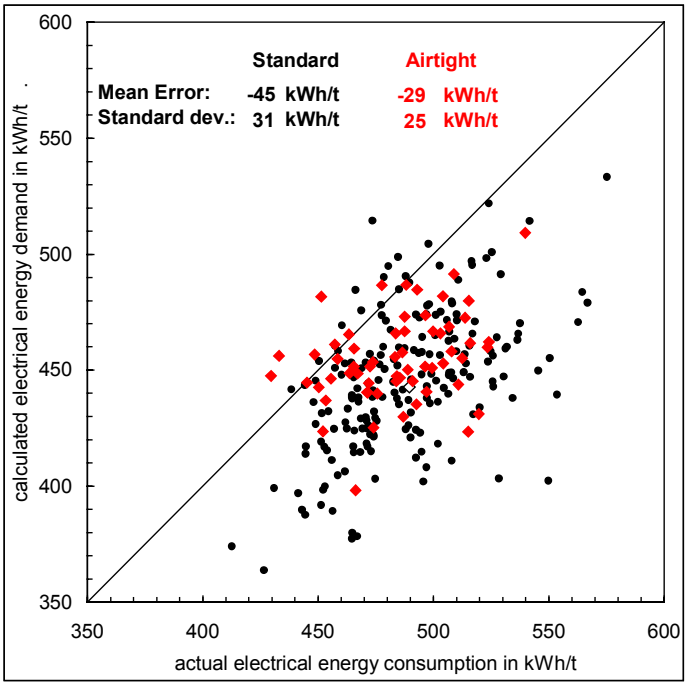

Fig. 4: Calculated versus actual electrical energy consumption for GMH heats

Off-gas measurement at the GMH furnace

To get a better understanding of the processes in the EAF, GMH got involved in developing a reliable continuous off-gas analysis many years ago. Today, it works very satisfactorily with an availability of about 95%. From the furnace a gas sample is drawn, dedusted and fed into a mass spectrometer (see **Fig. 5**). During every charging operation of the furnace, the gas sampling line is cleaned by purging with nitrogen. The gas sample is analysed for the concentrations of seven different species: CO, CO_2, H_2 and CH_4 are used to observe the progress of the combustion reactions. The analysed O_2 concentration serves as an indicator for the tightness of the sampling line, as for thermodynamical reasons the O_2 content in the furnace gas must be very low as soon as there is CO present in a substantial quantity. The analysis of the contents of N_2 and Ar provide the possibility to determine the total off-gas flow and the entrained air from the surroundings („false air“).

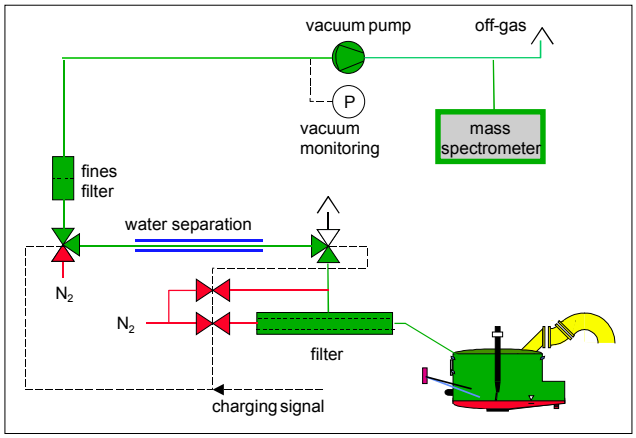

Fig. 5: Off-gas analysis at the GMH furnace

Fig. 6 displays the concentrations of O_2, CO, H_2 and CO_2 for a time period of 50 minutes of an example heat. The first 20 minutes show the meltdown period of the first scrap bucket. The O_2 concentration goes back to nearly zero as soon as a substantial CO content is present. The CO content itself fluctuates between 30 and nearly 50%. H_2 shows a peak of almost 50% in the beginning of the meltdown period which decreases rapidly. CO_2 barely reaches 10% except in the first two minutes. After the first meltdown phase, the second scrap bucket is charged. As mentioned before, during these 4 minutes of charging, the gas sampling line is purged with VSA-nitrogen, which explains the 4.5% oxygen analysed. The second meltdown period qualitatively is a repetition of the first, with a less extreme hydrogen peak at the beginning. After another 13 minutes, electric power and oxygen input are stopped briefly for taking a steel sample by a manually driven lance, which marks the end of the meltdown period. After sampling, the heat is superheated to the target tapping temperature of 1660°C.

During this process phase, the blowing of fine coal provides a foaming slag. However it is also the reason for CO concentrations well in excess of 40%. The time period displayed in Fig. 6 ends with the temperature measurement, which is also done with a manual lance and requires a brief interruption of the superheating process. Afterwards, the heat is tapped. Generally speaking, the utilisation of combustible matter during this example heat was not very good, as can be seen by the high contents of H_2 and CO throughout almost the whole process time. For the same time period, the off-gas flow and the flow of false air are displayed in **Fig. 7**. The off-gas flow fluctuates between 200 and 400 Nm³/min in the first five meltdown minutes, between 400 and 600 Nm³/min afterwards. Switching off the burners towards the end of the first meltdown phase results in a decrease of the off-gas flow rate from 600 back to 400 Nm³/min. Throughout the second meltdown and the superheating period, the off-gas flow fluctuates around 350 Nm³/min. The green curve displays the flow rate of entrained ambient air, which fluctuates between 100 and 200 Nm³/min, i.e. false air makes up for as low as roughly one third of the total off-gas volume. The red curve shows the off-gas temperature measured by means of a quotient pyrometer. It rises up to 1450 °C during meltdown, up to 1550°C in the superheating phase.

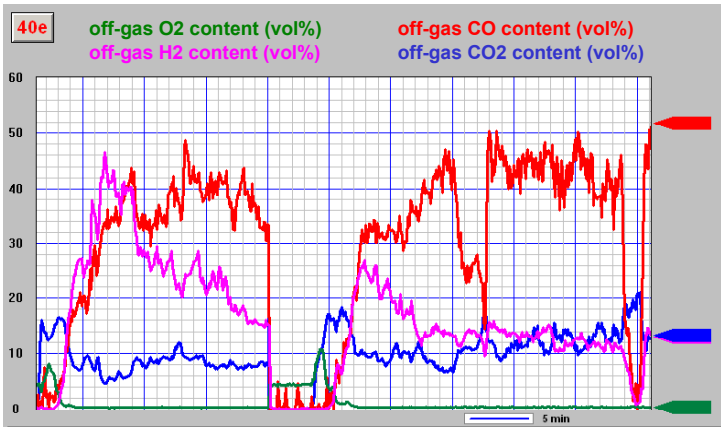

Fig. 6: Off-gas composition for an example heat

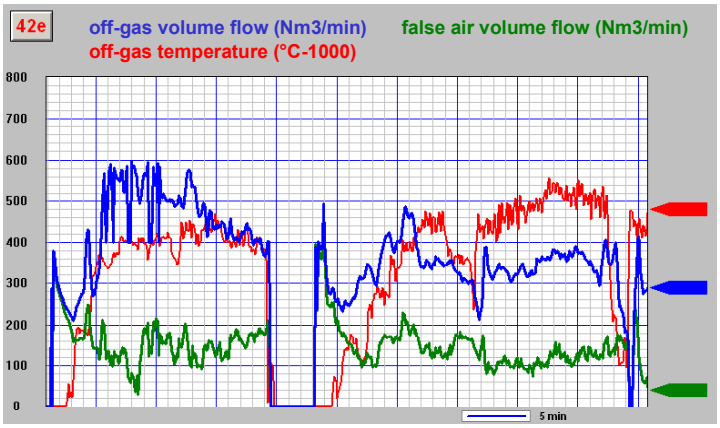

Fig. 7: Off-gas flow rate and temperature

Differential energy balance at the GMH furnace

These raw data are the basis to calculate the courses for some figures from the differential energy balance (**Fig. 8**). The electric power input appears more or less even at about 90 MW. The input that comes from chemical reactions fluctuates much more and covers a range of up to 50 MW. It includes the carbon and hydrogen combustion and the slag formation reactions. So the blue curve represents the total energy consumption, which is the sum of electric energy and reaction energy. Furthermore from the off-gas analysis is known, which energies leave the EAF unused as combustible matter, i.e. CO and H_2. During the first meltdown phase, this chemical energy of the off-gas reaches values of 80 MW in the top. **Fig. 9** shows the energy outputs of the process. The area below the green curve is the energy included in steel and slag. The area between green and brown curve represents the cooling water energy losses. The sensible heat of the off-gas is shown as area between brown and red curve. The blue curve, as in Fig. 8, represents the sum of all utilised energy inputs. Cooling water losses are low in the beginning of the meltdown phases, when scrap

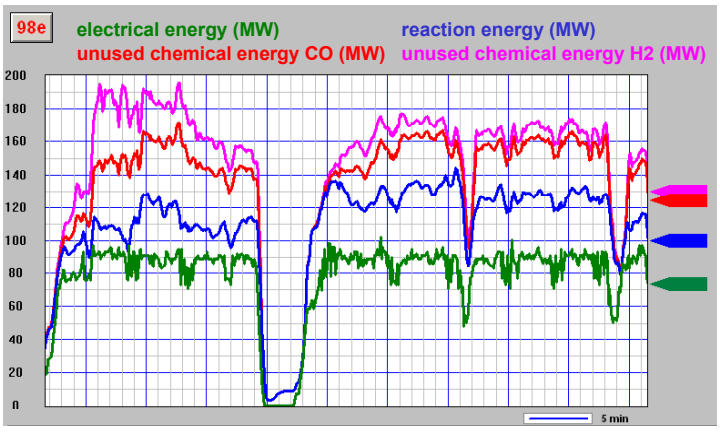

Fig. 8: Differential energy balance (Part I)

protects the furnace walls from arc radiation, and they increase with progress of meltdown. Sensible off-gas heat losses are mainly a function of the flow rate since the temperature fluctuations are limited.

From the raw data and the results of the energy balance which have been presented so far, the main information is distilled into one screen that is used to guide the process. The green curve in **Fig. 10** shows the accumulated energy in steel and slag, i.e. the integrated curve from Fig. 8. On reaching a target value, the temperature of the heat is measured and the heat is ready for tapping. The other information in the screen supports the furnace operators in reaching this point quickly. The blue curve shows the carbon post combustion ratio

$$\eta_{CO_2} = \frac{x_{CO_2}}{x_{CO} + x_{CO_2}}. \qquad (4)$$

Values of the ratio of around 20% through-out the largest part of the time show that, as already mentioned, the example heat had a rather poor utilisation of fossil fuels. The black curve integrates up the oxygen flow rate. The red curve, on the other hand, assesses the effectivity of oxygen utilisation in a very straight-forward way. It integrates the oxygen flow rate, weighted by the quotient of actual and target post combustion ratio.

$$V_{O_{2,eff}} = \int_{t=0}^{t} \dot{V}_{O_2,ges}(t) \cdot \frac{\eta_{CO2}(t)}{\eta_{CO2,target}} \qquad (5)$$

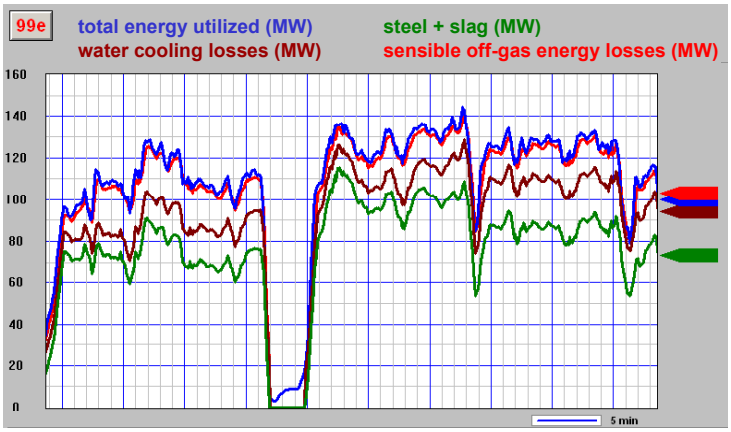

Fig. 9: Differential energy balance (Part II)

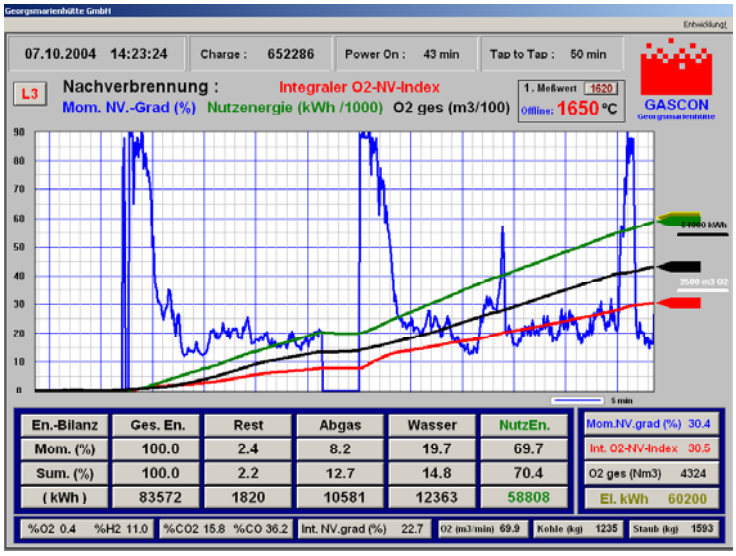

Fig. 10: Monitor of energy balance and post-combustion ratio

When the actual post combustion ratio matches its target value over the course of the heat, the red curve is congruent to the black. However, the example heat does not show a sufficient oxygen effectivity.

The bottom part of the screen shows the distribution of the energy consumed in useful energy (steel and slag), water cooling losses, sensible off-gas energy and other losses. Available are an integrated value in kWh, an integrated value in percent of total energy consumed and a momentary value in percent. 70% of the energy consumed for the example heat are useful energy, 15% heat up the cooling water and 13% are carried away with the off gas. The correlation between average post combustion ratio for a heat and energy utilization is depicted in **Fig. 11**. After equal electric energy input, heats with a high average PC ratio of 45% are 15 to 30°C hotter than heats with a low PC ratio of 28%. The energy released in the post combustion reactions obviously ends up as useful energy. It does not only heat up cooling water or off-gas.

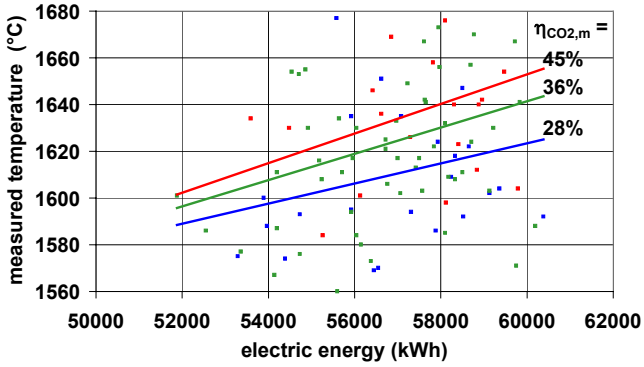

Fig. 11: Correlation between post combustion ratio and energy utilization

DEVELOPMENT OF A DYNAMIC ENERGY AND MATERIAL BALANCE MODEL

On the basis of the formula for the electrical energy demand, BFI developed a dynamic energy and mass balance model which can be used for on-line observation of the current EAF process state. In converting the influence parameters of the electrical energy demand formula into model parameters of a complete mass and energy balance model, results of a validation and evaluation of the influence parameters reported at the preceding Electric Steelmaking Conference in Venice [5] were taken into account. Furthermore a comprehensive study on the mass and energy balance of the GMH DC furnace [6] was considered. **Fig. 12** shows the structure of the BFI dynamic energy and mass balance model with the input values which are available at the GMH DC furnace.

The total weight (steel and slag) of the melt is calculated from the metallic materials and slag formers charged with the scrap baskets, and from the injected amount of dust. The specific meltdown energy of each charged scrap type is determined according to its contents of ferrous and non-ferrous components. Together with the specific meltdown energy of the slag formers, the totally required energy to melt down the charged materials and to heat up the melt to a reference temperature of 1600 °C is given. This calculation is comparable to the first line of the electrical energy demand formula shown in Table 1.

Additionally the effect of the hot heel in the furnace is considered in this calculation. Its amount is estimated from a simple mass balance at tapping of the preceding heat. The temperature of the hot heel at the beginning of the tap-to-tap time of the new heat is given by the tapping temperature of the preceding heat.

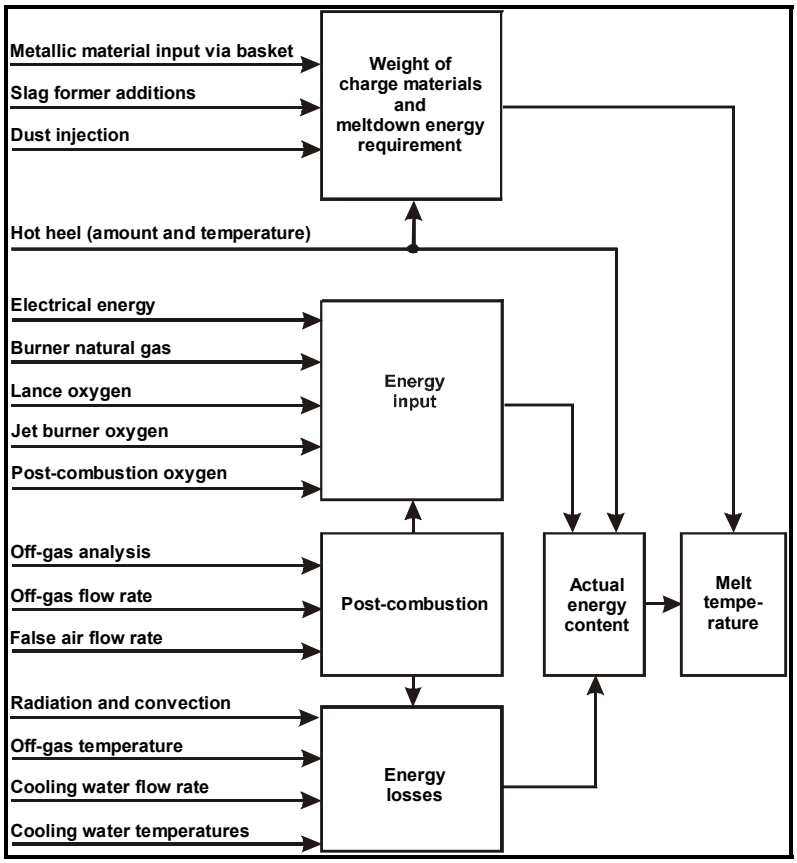

Fig. 12: Structure of the dynamic process model with input data available at the GMH DC-EAF

The energy input calculation comprises electrical and chemical energy, the latter one consisting of the energy input by burner natural gas, by oxygen input through lance and jet burners, and by injection of post-combustion oxygen. The flow rates of natural gas and oxygen are converted into a power input for the melt with theoretically achievable gain factors. This is different to the electrical energy demand formula, where values for the effective chemical energy input are applied which implicitly consider the energy losses by gas exhaustion. For natural gas the theoretical energy gain factor is given by the caloric energy of the combustion with oxygen. The supplied oxygen is consumed for different chemical reactions, e.g. decarburisation, oxidation of metals like silicon, manganese and iron, combustion of hydro-carbonates introduced by the scrap etc. As it is very difficult to determine the distribution of the oxygen to the different reactions for each heat individually, an average value for the energy gain by oxygen input was chosen.

The post combustion is derived from the measured off-gas values, taking into account the energy input by post combustion with oxygen coming from the false air, and the energy losses by the not completely combusted off-gas components CO, H_2 and CH_4. Further energy losses consist of the sensible heat of the off-gas, which is given by its flow rate and its temperature, and the thermal losses by the water-cooled panels, which are calculated from cooling water flow rate and the difference between inlet and outlet temperatures. Radiation losses occurring when the furnace roof is opened are calculated depending on the current melt temperature, and convection losses via the furnace hearth are taken into account with a fixed loss rate. The last two losses are considered in the electrical energy demand formula with the influence parameter for power-on and power-off time.

The difference between energy input and energy losses gives the actual energy content of the melt. Within this balance, also the hot heel with its energy content depending on its temperature has to be considered. To calculate the melt temperature, the actual energy content is related to the meltdown energy requirement. The energy input for superheating of the melt beyond the reference temperature of 1600°C is calculated with different specific heat values for steel and slag, which is similar to the consideration of the tapping temperature in the electrical energy demand formula.

The result of the dynamic mass and energy balance calculation is shown in **Fig. 13** for the GMH example heat which was already used in Fig. 6-10. In the upper part of the figure, the energy inputs by electrical energy, burner gas, lance and jet burner oxygen as well as post combustion are displayed as power versus time. In the middle part, the power losses due to the sensible and chemical heat of the off-gas, the water-cooled panels, as well as radiation and convection are shown.

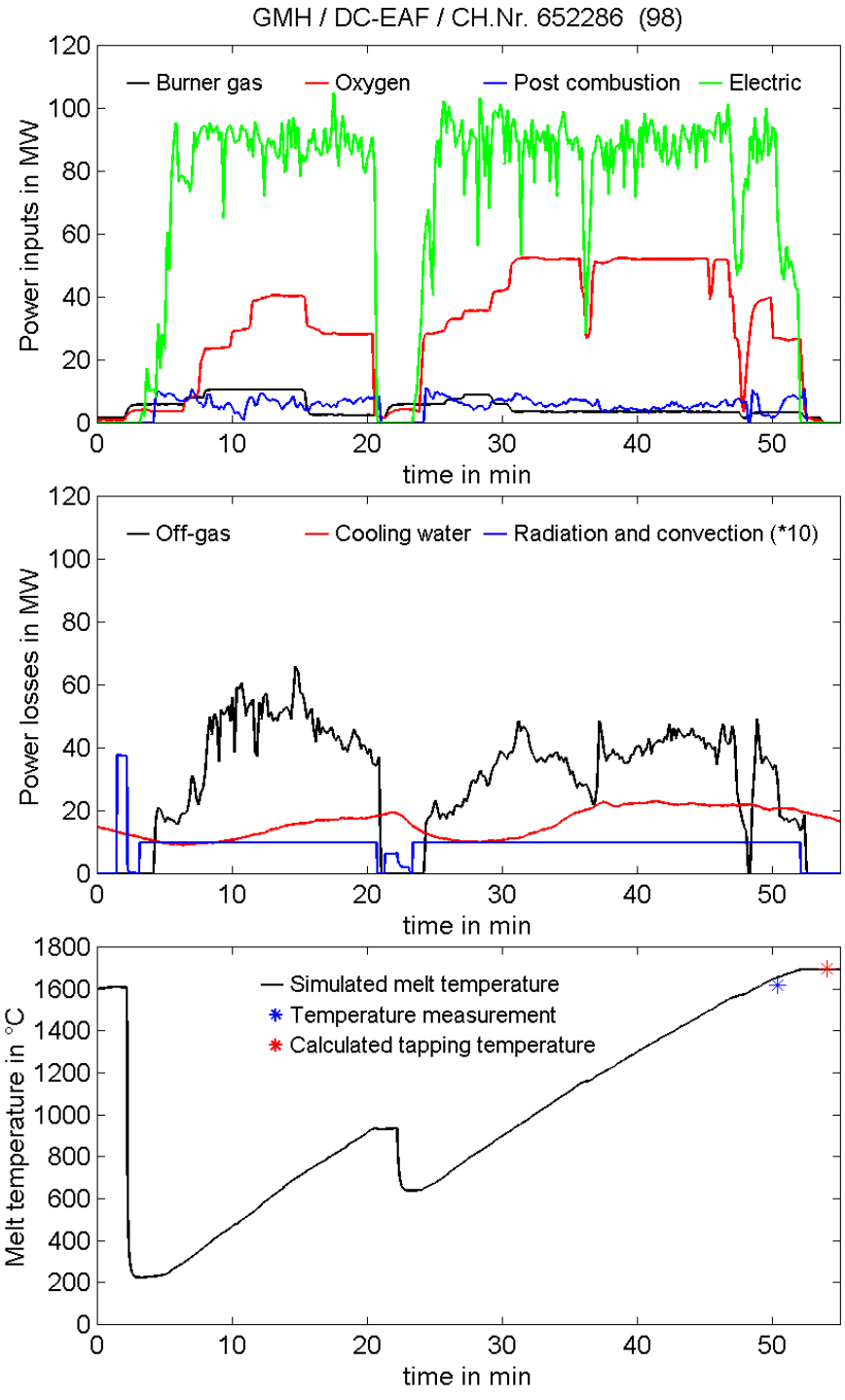

Fig. 13: Calculation result of the dynamic mass and energy balance model for the GMH example heat

Interesting is that the power loss by the exhaust gas is especially in the first meltdown phase at the same level as the power input by oxygen. This is due to the fact that especially in this phase a large amount of chemical energy is lost via the high contents of H_2 and CO in the off-gas.

The lower part of Fig.13 shows the calculated temperature of the melt. The times when the two buckets are charged are clearly indicated by the temperature drop. The simulated melt temperature is compared to the temperature measurement before tapping, and to a predicted tapping temperature, which is calculated with an empirical formula developed by GMH on the basis of the energy inputs which are performed after the temperature measurement. It can be seen that for this heat the correspondence between simulated and measured temperature is very good.

The accuracy of the dynamic process model regarding the calculation of the melt temperature was evaluated on the basis of a larger number of heats treated at the DC furnace of GMH. For the first temperature measurement after meltdown, an error standard deviation of 60 K, respectively converted into an energy value, of 13.8 kWh/t was achieved. With respect to the total energy input of around 690 kWh/t, this is a relative error of the energy balance of only 2 %, which is already a good accuracy. In comparison to the calculation with the electrical energy demand formula, the error standard deviation was almost cut in half.

CONCLUSIONS AND PROSPECTS

The comparison of different modelling approaches for the energy balance of an electric arc furnace has illustrated various aspects of application of such models. The electrical energy demand formula was used to evaluate and to judge different operation practices regarding the electrical energy consumption. A differential on-line energy balance based on measured off-gas values allows to follow the energetic efficiency of a furnace during treatment. In combination with a mass balance, the energy balance was used to built a complete dynamic model for the electric arc furnace, which can be used for on-line observation and control of the process. The dynamic EAF process model will be subject of improvement and extension in the future, and it will be used for on-line dynamic process control, e.g. regarding burners, oxygen injectors and post combustion.

REFERENCES

[1] Köhle, S.: Recent improvements in modelling energy consumption of electric arc furnaces. 7th European Electric Steelmaking Conference 2002, p. 1.305-1.314

[2] Improving the productivity of electric arc furnaces. ECSC Report EUR 20803, 2003

[3] Köhle, S.: Einflußgrößen des elektrischen Energieverbrauchs und des Elektrodenverbrauchs von Lichtbogenöfen. Stahl u. Eisen 112 (1992) No. 11, p. 59-67

[4] Köhle, S.: Rechnereinsatz zur Steuerung von Lichtbogenöfen. Stahl u. Eisen 100 (1980) No. 10, p. 522-528

[5] Pfeiffer, H.; Kirschen, M.: Thermodynamic analysis of EAF energy efficiency and comparison with a statistical model of electric energy demand. 7th European Electric Steelmaking Conference 2002, p. 1.413-1.428

[6] Kühn, R.: Untersuchungen zum Energieumsatz in einem Gleichstromlichtbogenofen zur Stahlerzeugung. Dissertation TU Clausthal, Shaker Verlag Aachen 2003

ACKNOWLEDGEMENTS

The research work concerning EAF modelling was partly performed within ECSC research projects. The authors like to thank the ECSC for their financial support.